Amendable decisions in living systems

Izaak Neri[1,2*†], Simone Pigolotti[3*†]

[1]Department of Mathematics, King's College London, Strand, London, WC2R 2LS, UK.

[2]Theoretical Sciences Visiting Program (TSVP), Okinawa Institute of Science and Technology Graduate University, Onna, 904-0495, Japan.

[3]Biological Complexity Unit, Okinawa Institute of Science and Technology Graduate University, Onna, 904-0495, Japan.

*Joint corresponding authors. Email: izaak.neri@kcl.ac.uk, simone.pigolotti@oist.jp .

†These authors contributed equally to this work.

A distinct feature of living systems is their capacity to take decisions based on uncertain environmental signals. Examples span from the microscopic scale of cells differentiating based on the concentration of a morphogene, to the macroscopic scale of decisions by animals or human beings. The current paradigm in decision theory is based on the assumption that decisions, once taken, cannot be revoked. However, living systems often amend their decisions if accumulated evidence favors an alternative hypothesis. In this paper, we develop a theory for amendable decision making in living systems. We find that, in contrast with irrevocable decisions, optimal amendable decisions can be taken in a finite average time at zero error probability. Our theory successfully predicts the outcome of a visual experiment involving human participants and the accuracy of cell-fate decisions in early development. These case studies demonstrate the broad applicability of the amendable decision paradigm in biology.

Living systems are able to make appropriate decisions based on signals received by their

environment. Examples can be found in animal behavior (*1*), such as in mate choice (*2*), foraging (*3, 4*), prey and predator detection (*5*), and selection of a nest site (*6, 7*). Performance in decision tasks has been extensively tested in laboratory experiments (*1, 4, 8, 9*). Being able to decide rapidly and appropriately is often a matter of life and death. For this reason, living systems are often argued to employ optimal decision strategies (*10, 11*).

We consider decision processes in which living observers have in mind different, mutually exclusive hypotheses about their environment. They then accumulate information about the environment, and store them in an internal representation called the evidence. At some point in time, they decide, based on the evidence, which of the hypotheses they believe to be correct.

The literature on biological decision making has predominantly focused on decisions that can not be revoked. In this case, the optimal decision strategy has been identified by Wald as the sequential probability ratio test (*12–14*). In this test, the evidence is constructed as the logarithm of the likelihood ratio of the two hypotheses, and a decision is taken as soon as the evidence reaches either a positive or a negative threshold. The sequential probability ratio test can be used as a normative model to rationalize fast decisions by animals and humans receiving perceptual stimuli (*15*). The activity of neurons in the parietal and prefrontal cortices that are involved with decisions indeed correlates with the likelihood ratio process (*11, 15–17*). The optimal decision strategy is characterized by speed-accuracy tradeoffs (*18*). For example, the average decision time increases as the similarity between the hypotheses is increased. Additionally, the average decision time increases as the error probability, i.e., the probability of committing for the wrong hypothesis, is decreased. Speed-accuracy tradeoffs have been confirmed in behavioral experiments on olfactory (*9*), visual (*3, 8*), and tactile (*19*) tasks performed by animals (*3, 7, 9, 19*) and humans (*8*); see (*1, 20*) for reviews.

Certain fast and accurate cellular processes, such as the expression of genes in response to morphogene signals (*10, 21–24*), T-cell activation in response to foreign ligands (*25*), and stem cell differentiation (*26*) can be conceptualized as decisions as well (*27–29*). The sequential probability ratio test has also been applied to this kind of decisions (*24, 29*). A classic example of a cell-fate decision is the expression of the gap gene Hunchback by nuclei in the embryo of the fruit fly *Drosophila melanogaster* in response to the morphogen Bicoid (*10, 28*). These nuclei decide whether to express Hunchback in about 10-20 minutes, about one order of magnitude faster (*10, 30*)

than the estimated lower limit of about 2 hours set by the Berg-Purcell bound (*31*).

Irrevocable decisions are often unnatural for living beings. Perceptual studies have shown that humans often change their mind after having perceived a stimulus and taken a decision, thereby lowering their error probability (*32–34*). It is also debatable whether cellular decisions are irrevocable. For example, in vivo imaging of the Bicoid-Hunchback system show that Hunchback can switch its expression level several times in a nuclear cycle (*35*). More in general, one might argue that the dynamics of subcellular regulatory systems responsible of decisions gradually converge towards one of the outcome states, rather than in a sudden irreversible transition (*36–38*).

In this paper, we propose a theory for decision processes in which, after decisions, observers maintain their right to change their mind, should additional evidence overwhelmingly favor the alternative hypothesis. We identify the optimal strategy in this scenario. In stark contrast with irrevocable decisions, the optimal amendable strategy is characterized by a vanishing error probability in a finite average decision time. We performed a human perception study to compare amendable and irrevocable decision, finding support our theoretical predictions. We also propose an amendable decision model for the Bicoid-Hunchback system. Our model successfully predicts the experimentally measured Hunchback profile without adjustable parameters.

Results

Irrevocable versus amendable decisions

We focus on decisions entailing two different hypotheses, + and −, on a certain phenomenon. An observer acquires information about this phenomenon by perceiving a time-dependent signal $X(t)$, see Fig. 1A. This signal is usually noisy; its statistics depend on which of the two hypotheses holds. The observer monitors the signal and stores the information contained in it into a time-dependent variable $E(t)$, called the evidence. The evidence is constructed so that positive and negative values of E represent accumulated evidence supporting hypothesis + and −, respectively. The decision is a binary variable $D \in (+, -)$ that depends on the evidence and is considered correct if it matches the hypothesis.

Irrevocable and amendable processes differ in the nature of decisions. In an irrevocable decision,

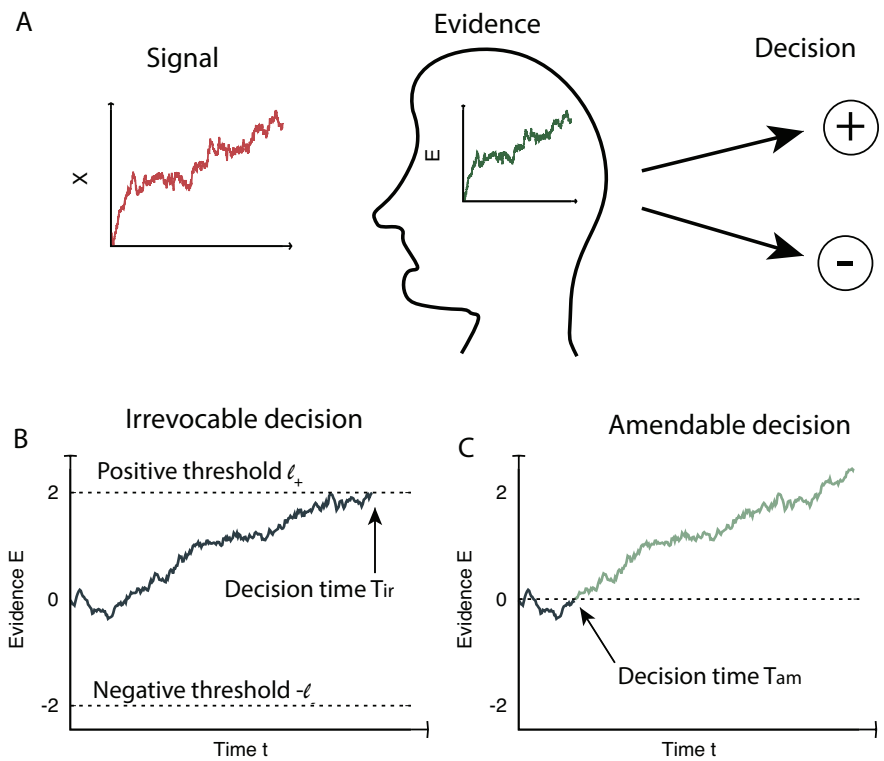

Figure 1: (A) Biological decision making. An environmental signal is observed by a living being, that stores the information contained in it in a process called the evidence. After having accumulated enough information, the observer takes a binary decision. (B) Irrevocable decision making. The observer commits to the + or - hypothesis as soon as the evidence crosses a positive or negative threshold, respectively. This commitment is irreversible. (C) Amendable decision making. In this case, the observer is in favor of the + or − hypothesis whenever $E(t)$ is greater or smaller than zero, respectively. A final decision time can be identified a posteriori as the moment when the evidence process crosses zero for the last time.

the observer commits to the hypothesis + (or −) as soon as the collected evidence crosses either a positive threshold ℓ_+ or a negative threshold $-\ell_-$, see Fig. 1B. This idea is at the basis of Wald's sequential test (*12, 13*). This commitment is final. The decision time $T_{\rm ir}$ is the time at which either of the threshold is crossed. Properties of irrevocable decision processes can be calculated using the theory of first-passage times (*39*). Choosing larger thresholds amounts to safer decisions, i.e., a lower probability of committing to the wrong hypothesis. However, this comes at a cost of a longer decision time.

In an amendable decision process, observers can alter their choice, so that their decision is only tentative at any time during the observation. We call $d(t) \in (+, -)$ the tentative decision at time t. A natural strategy is to set $d(t)$ equal to the sign of $E(t)$. In practice, the evidence $E(t)$ can change sign several times, leading to the same number of amendments to the tentative decision. However, even if observers have unlimited available time, after a certain time the accumulated evidence may be so overwhelming that they will never change opinion again. Alternatively, one could consider scenarios in which observers have a finite available time $t_{\rm f}$ to reach a decision. We define the final decision D as the large-time limit of $d(t)$ in the infinite-time case, or as $d(t_{\rm f})$ in the finite-time case. We also identify a posteriori a decision time $T_{\rm am}$ as the time at which the evidence process crosses zero for the last time, see Fig. 1C.

Drift-diffusion

Our first example are signals whose statistics are described by a drift-diffusion process

$$\frac{dX}{dt} = \mu_\pm + \sigma\, \xi(t)\,, \tag{1}$$

where μ_+ and μ_- are the drift coefficients corresponding to the two hypotheses and $\xi(t)$ is white noise. Without loss of generality, we set $\mu_+ > \mu_-$. We express the dynamics of the evidence process by

$$\frac{dE}{dt} = \pm\gamma + \xi(t)\,, \tag{2}$$

where the plus/minus sign of the drift term depends on which of the two hypotheses holds, and γ is the average rate of acquisition of evidence. In (2), we have set the amplitude of the noise equal to one by an appropriate choice of the units of E.

For an irrevocable decision based on the Wald test, the optimal choice of evidence is given by the likelihood ratio $E(t) \propto \ln P(X(t)|+)/P(X(t)|-)$. Here, $P(X(t)|+)$ and $P(X(t)|+)$ are the probabilities of $X(t)$ given the positive and negative hypothesis, respectively. This choice is optimal, in the sense of minimizing the average irrevocable decision time at a given error probability (see (*40*)). For the evidence defined in this optimal way, one has $\gamma = \gamma_{\rm opt} = 1/(2\sqrt{\tau})$, where we have introduced the characteristic time $\tau = \sigma^2/(\mu_+ - \mu_-)^2$. The initial condition depends on the initial prior on the two hypotheses. Throughout this paper, we shall assume that the two hypotheses are equally likely, so that the optimal initial condition is $E(0) = 0$. Under this assumption, we have characterized the optimal strategy for amendable decisions and found that the log-likelihood ratio evidence process is also optimal in this case.

We first compare the average decision time in the two setups for the optimal evidence, see Fig. 2A. In the irrevocable case, the average decision time depends on the choice of the thresholds, and thus on how the observer trades off speed and error probabilities. In particular, for small error probabilities η, the average decision time scales as $\langle T_{\rm ir}\rangle \sim -\log(\eta)$. In contrast, amendable decisions are error-free. The average amendable decision time is expressed by

$$\langle T_{\rm am}\rangle = 4\tau \,. \tag{3}$$

In this case, although the error probability vanishes, $\langle T_{\rm am}\rangle$ remains finite. Amendable decisions are also faster than irreversible decisions, unless the observer is willing to accept an error probability larger than a critical value $\eta_c \approx 0.08$. While the distribution $p_{\rm ir}(t)$ of irrevocable decision time presents a peak at intermediate time, the distribution of amendable decision times

$$p_{\rm am}(t) = \frac{1}{\sqrt{8\pi t\tau}} \exp\left(-\frac{t}{8\tau}\right) \,. \tag{4}$$

monotonically decreases under our conditions, see Fig. 2B.

So far, we have considered cases in which the time available to the observer is unlimited. However, in practical situations, the observer might be forced to make a call within a certain maximum time $t_{\rm f}$. In such settings, amendable decisions are characterized by a finite error probability, see Fig. 2C and Methods. For small $t_{\rm f}$, the distribution of decision times presents a bimodal shape, see Fig. 2D and Methods.

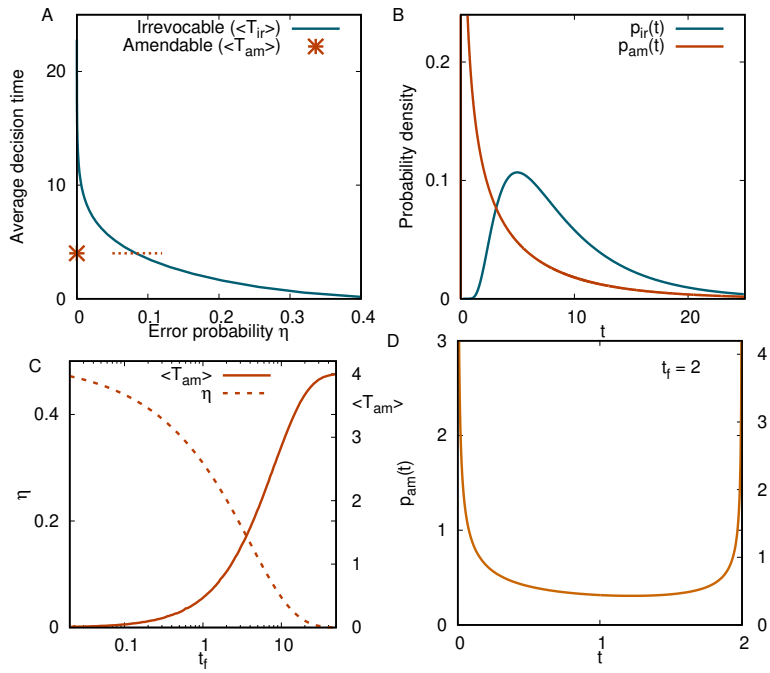

Figure 2: Amendable and irrevocable decisions for the drift-diffusion process. The evidence process is governed by (2) with $\gamma = \gamma_{\text{opt}} = 1/(2\sqrt{\tau})$ and $\tau = 1$. (A) Comparison of average decision times. In the irrevocable case, the decision time depends on the error probability η, while amendable decisions are always error-free ($\eta = 0$). Irrevocable decisions are faster for $\eta < \eta_c \approx 0.083$. (B) Decision time distributions for amendable and irrevocable decisions for infinitely large observation time t_{f}. In the irrevocable case, we have set $\eta = 0.01$. (C) Average decision time and error probability for a finite observation time, $t \in [0, t_{\text{f}}]$. (D) Distribution of amendable decision times for a finite observation time.

Amendable vs. irreversible decisions in a visual perception experiment

We performed an experiment with human participants. Participants were asked to observe the motion of a randomly moving dot on a screen, and assess whether the motion is biased towards the left or right direction by pressing a key. In the irrevocable version of the task, pressing a key terminated the game. In the amendable version, participants could alter their decision an arbitrary number of times, until a time limit $t_{\text{f}} = 10$s. At the initial time, the tentative decision $d(t)$ was randomly initialized to $+$ or $-$ with equal probabilities. Both in the irrevocable and amendable version, participants played four different versions of the games of increasing difficulty, i.e., reduced bias. Participants were

instructed to decide as fast as possible, but without making too many mistakes.

In keeping with the literature, we model evidence accumulation as a drift-diffusion process. We consider both an optimal (normative) model (*41*) in which we set the evidence rate to its optimal value ($\gamma = \gamma_{\text{opt}}$) and a descriptive model in which we infer γ from the experimental data. The optimal evidence rate is determined by the drift and diffusion coefficients characterizing the dot motion. Therefore, the optimal amendable decision model has no fitting parameters. In contrast, the threshold ℓ is a free parameter for the optimal irrevocable decision model.

As predicted by the optimal model, amendable decisions are error-free, at least when the task is not too difficult (Fig. 3A). In the hardest version of the game, errors take place. This can be explained within the optimal model because of the finite duration of each trial (see Methods). In contrast, irrevocable decisions are error-prone for all game difficulties, and characterized by a speed-error tradeoff (Fig. 3A).

For the descriptive model, we estimated the evidence rate γ for each participant and each game (Fig. 3B). In most cases, these estimates are smaller than the optimal evidence rate, as expected. Estimates in irrevocable and amendable games are broadly compatible. In most cases, evidence rates are higher in amendable than in irrevocable games, and therefore closer to the optimal ones. For each of the games, tradeoffs curves calculated for the evidence rate averaged over the participants are in good agreement with participants performance (dashed lines in Fig. 3A).

We next compare the empirical distributions of decision times with those of the optimal model. For easy games, the empirical distributions present a "gap" for short times (on the order of 0.1s) compared with the theoretical prediction, see Fig. 3C. This discrepancy is likely due to the finite response time of players. The tail of the distribution is instead in quantitative agreement with the theoretical one. For harder games, we find an excellent agreement between the theory and the experiment for all times. This is consistent with the observation that the empirical drift is close to the optimal ones for these games, suggesting that players adopt a nearly optimal strategy. Empirical decision times distributions for irrevocable games are qualitatively different than those for amendable ones, with a distinct peak at intermediate times as predicted by the theory (Fig. 3D). Also in this case, the quantitative agreement between the theory and the experimental data improves for harder games.

Amendable decisions in cellular sensing

Biological cells often need to accurately measure the concentration of a molecule, for example, an extracellular ligand or a nuclear transcription factor, and take decisions according to the value of the concentration. The observer is a spherical body that absorbs molecules present in a surrounding fluid at concentration c_∞ far from itself, see Fig. 4A. We assume that the environment is at thermodynamic equilibrium, so that the stationary current of absorbed molecules is given by $j = 4\pi r D c_\infty$, where r is the radius of the observer and D the molecular diffusion coefficient (*31*).

We consider the task of distinguishing between two values of the concentration, c_∞^+ and c_∞^-, corresponding to two different rates j_+ and j_-, respectively. Without loss of generality, we assume $c_+ > c_-$. The number of molecules absorbed in a time interval $[0, t]$ is given by a Poisson process $N_\pm(t)$ of rate $j_\pm$. This process represents our observation process. The precision parameter $\epsilon = (c_+ - c_-)/c_+ = (j_+ - j_-)/j_+$, quantifies the relative difference between the two concentrations, and therefore the difficulty of the discrimination task.

Also in this case, the optimal choice of the evidence is given by the likelihood ratio process (*12*). This optimal evidence is governed by

$$\frac{dE}{dt} = -\frac{\epsilon}{\tau} + \ln\left(\frac{1}{1-\epsilon}\right)\frac{dN_\pm}{dt} \tag{5}$$

where $\tau = 1/j_+$, see Methods and (*29*).

We compare the average decision time using the amendable and the irrevocable approach, see Fig 4B. In both cases, the average decision time scales as ϵ^{-2}, as in the Berg-Purcell theory. Also in this case, the irrevocable decision time depends on the chosen error rate η, while amendable decisions are error-free. Remarkably, the ratio between the irreversible and amendable is nearly independent of the precision ϵ (see Methods). In particular, amendable decisions are faster for $\eta < 0.08$ approximately, as in the drift-diffusion case, independently of the precision ϵ.

Mathematical analysis of receptor models often approximate the input signal as a drift-diffusion process (*29*). For amendable decisions, we compute the distribution of decision times without resorting to such approximation. The solution show how the quantized nature of the information obtained from incoming molecules affects the statistics of the decision time. We indeed find that the distribution of decision time is characterized by a rich structure, which is markedly different depending on whether the plus or minus hypothesis holds. In particular, for the positive hypothesis

(higher concentration), the distribution presents a sawtooth shape (Fig. 4C). In contrast, for the negative hypothesis, the distribution is nonzero only over a discrete set of times (Fig. 4D). This difference is due to an asymmetry in the evidence dynamics embodied in (5): the evidence increases in discrete steps whenever the observer absorbs a molecule, while gradually declining in time intervals when no molecule is received.

Cell-fate decisions induced by morphogen gradients

In the early development of multicellular organisms, the embryo is patterned by the expression of certain genes based on their spatial location. We consider the Bicoid-Hunchback system in the fruit fly. During the nuclear cycles 9 to 13 of the fruit fly development, the transcription factor Bicoid forms an exponentially decaying expression profile along the anterior-posterior axis of the embryo (*10, 30, 42*). Hunchback is a gene activated by Bicoid that develops an on-off expression profile depending on whether nuclei belong to the anterior or posterior half of the embryo, respectively (*42, 43*), see Fig. 5A. Live imaging of nascent RNA transcription reveals that nuclei in the posterior half are capable of switching off Hunchback expression following a transient activation, consistent with the amendable decision model (*35, 44*). To apply our theory to this system, we assume that nuclei are optimized for distinguishing the concentration differences experienced by neighboring nuclei at the point along the embryo axis where Hunchback switches its expression (see Fig. 5A and Methods).

The amendable decision model is able to generate a sharp Hunchback profile in a timescale compatible with that of nuclear cycles, see Fig. 5B. The predicted optimal profile is in excellent quantitative agreement with the experimentally measured one in the wild type fruit fly (*43*), without fitting parameters, in agree with the idea that the system operates in an optimal way. In contrast, a model based on irrevocable decision leads to much less sharp profiles, regardless of the choice of the decision thresholds (Fig. 5C). The predicted optimal decision times are in the order of minutes, and decrease with the distance from the boundary (Fig. 5D), in qualitative agreement with experiments (*44*).

Discussion

In this paper, we have shown that amendable decisions are governed by different laws than irrevocable ones. In particular, at variance with irrevocable decisions, amendable decisions can be taken in a finite average time at zero error probability. The theory presented here constitutes a paradigm with broad applicability in biology.

We have demonstrated the practical difference between amendable and irrevocable decision in a visual perception experiment, inspired to classic studies (*8, 45*). Despite being a small-scale study, our experiments confirmed the salient predictions of our theory. In addition, the estimated evidence rate in amendable tasks tended to be larger in absolute values, and therefore closer to optimality, than in irrevocable ones. This supports that amendable decision tasks can more accurately capture the rate of acquired information in perception experiments. As a future perspective, it might be interesting to devise more detailed models of human amendable decision process, for example taking into account a finite response time in perception and in changing opinion.

The theory of amendable precision provides a fresh perspective on the classical biophysical problem of sensing a concentration at the subcellular scale. In particular, applied to the Bicoid-Hunchback system in the fruit fly, the amendable decision model predicts a decision profile along the embryo in excellent quantitative agreement with experimental data and without fitted parameters. In contrast, the irrevocable model requires setting a threshold and predicts a shallow decision profile that does not match the experiments. This discrepancy can be resolved by assuming that Bicoid cooperatively binds to multiple Hunchback promoter sites (*24*). Overall, the amendable model provides a more parsimonious explanation for the experimental observations. An interesting future perspective is to study biomolecular mechanisms that could implement an amendable decision process in a nucleus.

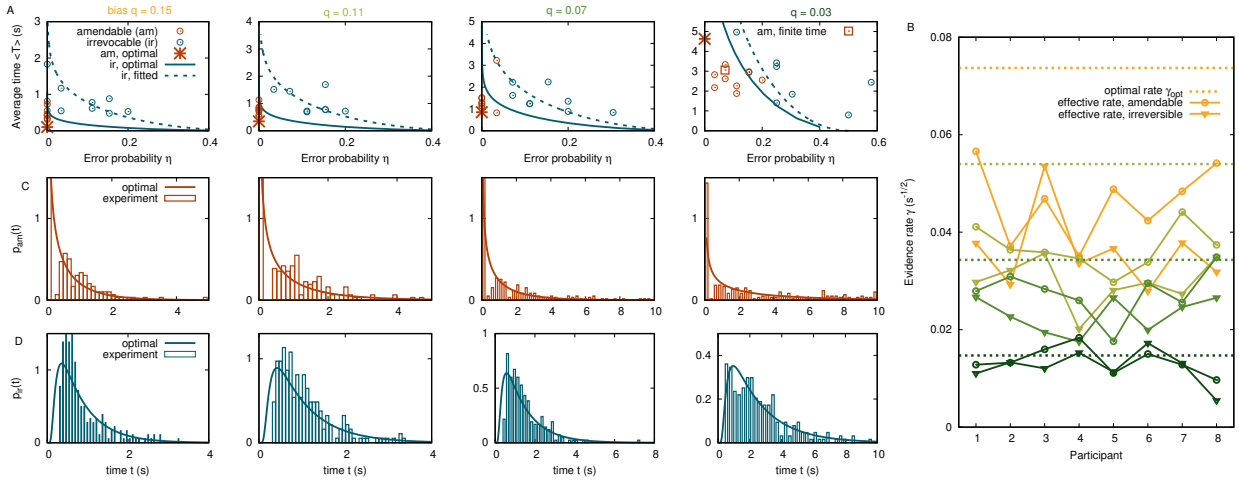

Figure 3: Amendable vs. irreversible decisions in a visual perception experiment. (A) Speed-error tradeoffs for the four game difficulties. The game difficulty is determined by the bias parameter q (see Methods). Circles represent error probability and decision time averaged for each individual player. In the irrevocable cases, average decision times and error probabilities are characterized by a tradeoff (Pearson correlation coefficients among participants $r = (-0.68, -0.48, -0.61, -0.61)$ from left to right). The star and the continuous line mark the optimal strategies in the amendable and irrevocable case respectively (see Fig. 2A). In the optimal case, the parameter γ_{opt} is computed from the drift and diffusion of the moving dot (see Methods). The dashed lines represent the irrevocable strategy associated with the fitted evidence rate γ (see Methods). For $q = 0.03$, the square marks the optimal finite-time amendable strategy (see Methods). For all the other game difficulties, the finite-time amendable strategy is practically indistinguishable from the infinite-time one. (B) Estimates of the rate of evidence acquisition γ for all players and all games (see Methods), compared with the optimal evidence rates γ_{opt}. (C) Empirical distributions of the amendable decision time $p_{\text{am}}(t)$ from experiments, compared with the decision-time distribution for the optimal evidence process given by (4). (D) Empirical distributions of the irrevocable decision time $p_{\text{am}}(t)$ from experiments, compared with the optimal distribution estimated from the empirical values of η (see Methods).

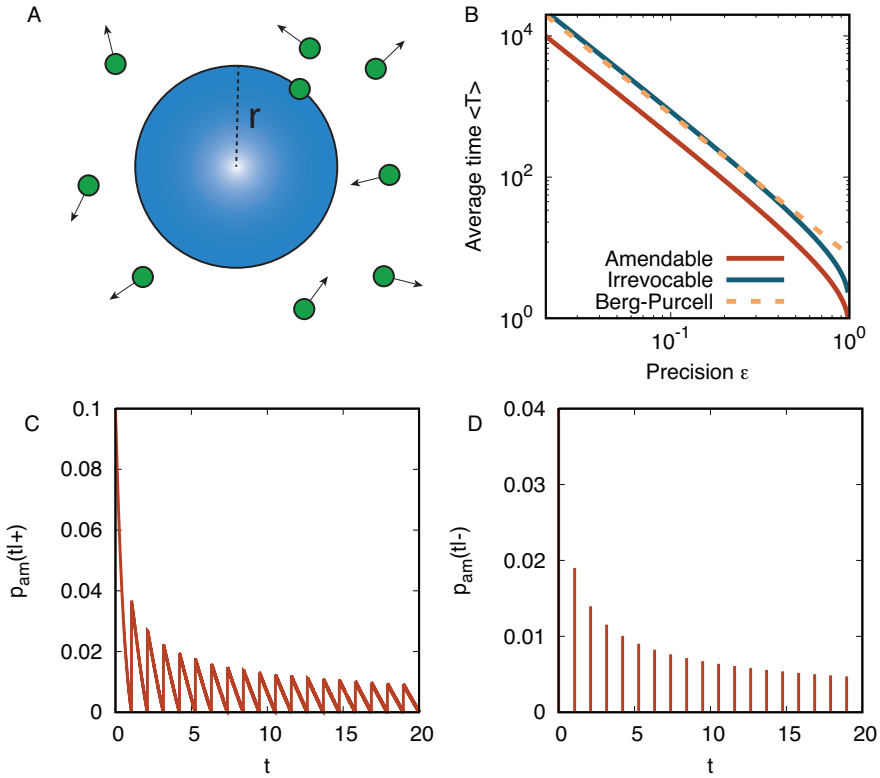

Figure 4: Decisions in molecular sensing. (A) A microscopic observer absorbs molecules from the environment attempting to detect their concentration. (B) Average decision time as a function of the precision ϵ. We have set $\tau = 1$. The Berg-Purcell line represent an estimate based on the root mean square fractional error in the determination of the concentration, $\langle T \rangle = (4\pi/(1.61))\epsilon^{-2}$, see Eq. (30) in (*31*). In the irrevocable case, we have set $\eta = 0.01$. (C) Distribution of amendable decision times for the + hypothesis and $\epsilon = 0.1$. (D) same as (C), but for the − hypothesis. The distribution is discrete in this case (see Methods).

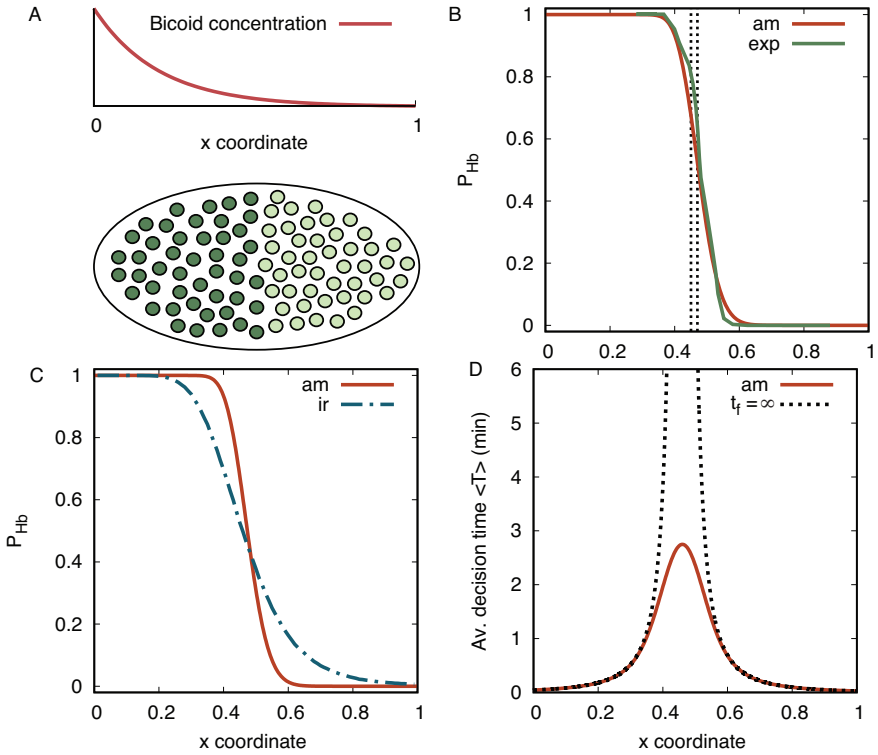

Figure 5: Amendable decisions in the Bicoid-Hunchback system (A) The Bicoid-Hunchback system in the *Drosophila* embryo. Bicoid is a morphogene that forms a longitudinal concentration gradient along the embryo. Nuclei sense the Bicoid concentrations and decide whether to express Hunchback (green circles) or not (light circles). (B) Probability $P_{\mathrm{H}b}$ to express Hunchback at the end of the nuclear cycle as a function of the rescaled coordinate x. Parameters are chosen based on experimental observations (see Methods). Experimental data represent the relative number of nuclei that that express nascent RNA transcripts of the Hunchback gene, as detected with fluorescent in situ hybridization in the 10th nuclear cycle of the wild type fruit fly (taken from Figure 3 of Ref. (*43*)). The two dotted vertical lines mark the separation between two neighboring nuclei at the Hunchback interface. (C) Comparison between amendable and irrevocable decisions for $t_{\mathrm{f}} = 10$min. For the irrevocable case, we have set $\ell_+ = 0.07$ and $\ell_- = 10$ as these value minimize the distance to the experimental curve. In cases where neither of the thresholds have been reached at the final time, we assumed that cells do not express Hunchback, as in the case in which the negative threshold is reached. (D) Average amendable decision time using the continuous approximation for $t_{\mathrm{f}} = 5.5$min compared with the case $t_{\mathrm{f}} = \infty$.

References and Notes

1. L. Chittka, P. Skorupski, N. E. Raine, Speed–accuracy tradeoffs in animal decision making. *Trends in ecology & evolution* **24** (7), 400–407 (2009).

2. P. R. Backwell, N. I. Passmore, Time constraints and multiple choice criteria in the sampling behaviour and mate choice of the fiddler crab, Uca annulipes. *Behavioral Ecology and Sociobiology* **38**, 407–416 (1996).

3. L. Chittka, A. G. Dyer, F. Bock, A. Dornhaus, Bees trade off foraging speed for accuracy. *Nature* **424** (6947), 388–388 (2003).

4. H. MaBouDi, J. A. Marshall, N. Dearden, A. B. Barron, How honey bees make fast and accurate decisions. *Elife* **12**, e86176 (2023).

5. L. Chittka, D. Osorio, Cognitive dimensions of predator responses to imperfect mimicry. *PLoS Biology* **5** (12), e339 (2007).

6. K. M. Passino, T. D. Seeley, Modeling and analysis of nest-site selection by honeybee swarms: the speed and accuracy trade-off. *Behavioral Ecology and Sociobiology* **59**, 427–442 (2006).

7. N. Stroeymeyt, M. Giurfa, N. R. Franks, Improving decision speed, accuracy and group cohesion through early information gathering in house-hunting ants. *PLoS one* **5** (9), e13059 (2010).

8. R. Ratcliff, G. McKoon, The diffusion decision model: theory and data for two-choice decision tasks. *Neural computation* **20** (4), 873–922 (2008).

9. D. Rinberg, A. Koulakov, A. Gelperin, Speed-accuracy tradeoff in olfaction. *Neuron* **51** (3), 351–358 (2006).

10. T. Gregor, D. W. Tank, E. F. Wieschaus, W. Bialek, Probing the limits to positional information. *Cell* **130** (1), 153–164 (2007).

11. S. Kira, T. Yang, M. N. Shadlen, A neural implementation of Wald's sequential probability ratio test. *Neuron* **85** (4), 861–873 (2015).

12. A. Wald, Sequential tests of statistical hypotheses. *Ann. Math. Statist.* **16** (2), 117–186 (1945).

13. J. L. Melsa, D. L. Cohn, *Decision and estimation theory* (McGraw-Hill) (1978).

14. A. Tartakovsky, I. Nikiforov, M. Basseville, *Sequential analysis: Hypothesis testing and change-point detection*, vol. 136 of *Monographs on statistics and applied probability* (CRC press) (2015).

15. J. I. Gold, M. N. Shadlen, The neural basis of decision making. *Annu. Rev. Neurosci.* **30** (1), 535–574 (2007).

16. M. N. Shadlen, W. T. Newsome, Neural basis of a perceptual decision in the parietal cortex (area LIP) of the rhesus monkey. *Journal of neurophysiology* **86** (4), 1916–1936 (2001).

17. X.-J. Wang, Decision making in recurrent neuronal circuits. *Neuron* **60** (2), 215–234 (2008).

18. N. Uchida, A. Kepecs, Z. F. Mainen, Seeing at a glance, smelling in a whiff: rapid forms of perceptual decision making. *Nature Reviews Neuroscience* **7** (6), 485–491 (2006).

19. H. Kaneko, H. Tamura, T. Kawashima, S. S. Suzuki, A choice reaction-time task in the rat: a new model using air-puff stimuli and lever-release responses. *Behavioural brain research* **174** (1), 151–159 (2006).

20. R. Bogacz, E.-J. Wagenmakers, B. U. Forstmann, S. Nieuwenhuis, The neural basis of the speed–accuracy tradeoff. *Trends in neurosciences* **33** (1), 10–16 (2010).

21. L. Wolpert, Positional information and the spatial pattern of cellular differentiation. *Journal of theoretical biology* **25** (1), 1–47 (1969).

22. H. L. Ashe, J. Briscoe, The interpretation of morphogen gradients. *Development* **133**, 385–394 (2006).

23. M. Ibanes, J. C. I. Belmonte, Theoretical and experimental approaches to understand morphogen gradients. *Molecular Systems Biology* **4** (1), 176 (2008).

24. J. Desponds, M. Vergassola, A. M. Walczak, A mechanism for hunchback promoters to readout morphogenetic positional information in less than a minute. *Elife* **9**, e49758 (2020).

25. P. François, G. Voisinne, E. D. Siggia, G. Altan-Bonnet, M. Vergassola, Phenotypic model for early T-cell activation displaying sensitivity, specificity, and antagonism. *Proceedings of the National Academy of Sciences* **110** (10), E888–E897 (2013).

26. C. Li, J. Wang, Quantifying cell fate decisions for differentiation and reprogramming of a human stem cell network: landscape and biological paths. *PLoS computational biology* **9** (8), e1003165 (2013).

27. T. J. Kobayashi, Implementation of dynamic Bayesian decision making by intracellular kinetics. *Physical review letters* **104** (22), 228104 (2010).

28. G. Balázsi, A. Van Oudenaarden, J. J. Collins, Cellular decision making and biological noise: from microbes to mammals. *Cell* **144** (6), 910–925 (2011).

29. E. D. Siggia, M. Vergassola, Decisions on the fly in cellular sensory systems. *Proceedings of the National Academy of Sciences* **110** (39), E3704–E3712 (2013).

30. T. Gregor, E. F. Wieschaus, A. P. McGregor, W. Bialek, D. W. Tank, Stability and nuclear dynamics of the bicoid morphogen gradient. *Cell* **130** (1), 141–152 (2007).

31. H. C. Berg, E. M. Purcell, Physics of chemoreception. *Biophysical journal* **20** (2), 193–219 (1977).

32. A. Resulaj, R. Kiani, D. M. Wolpert, M. N. Shadlen, Changes of mind in decision-making. *Nature* **461** (7261), 263–266 (2009).

33. R. van Den Berg, *et al.*, A common mechanism underlies changes of mind about decisions and confidence. *Elife* **5**, e12192 (2016).

34. C. Stone, J. B. Mattingley, D. Rangelov, On second thoughts: changes of mind in decision-making. *Trends in Cognitive Sciences* **26** (5), 419–431 (2022).

35. H. G. Garcia, M. Tikhonov, A. Lin, T. Gregor, Quantitative imaging of transcription in living Drosophila embryos links polymerase activity to patterning. *Current biology* **23** (21), 2140–2145 (2013).

36. S. Huang, G. Eichler, Y. Bar-Yam, D. E. Ingber, Cell fates as high-dimensional attractor states of a complex gene regulatory network. *Physical review letters* **94** (12), 128701 (2005).

37. M. Mojtahedi, *et al.*, Cell fate decision as high-dimensional critical state transition. *PLoS biology* **14** (12), e2000640 (2016).

38. F. Corson, E. D. Siggia, Gene-free methodology for cell fate dynamics during development. *Elife* **6**, e30743 (2017).

39. S. Redner, *A guide to first-passage processes* (Cambridge university press) (2001).

40. A. Wald, J. Wolfowitz, Optimum character of the sequential probability ratio test. *The Annals of Mathematical Statistics* pp. 326–339 (1948).

41. E. J. Johnson, R. Ratcliff, Computational and process models of decision making in psychology and behavioral economics, in *Neuroeconomics*, P. W. Glimcher, E. Fehr, Eds. (Elsevier), chap. 3, pp. 35–47, 2nd ed. (2014).

42. B. Houchmandzadeh, E. Wieschaus, S. Leibler, Establishment of developmental precision and proportions in the early Drosophila embryo. *Nature* **415** (6873), 798–802 (2002).

43. A. Porcher, *et al.*, The time to measure positional information: maternal hunchback is required for the synchrony of the Bicoid transcriptional response at the onset of zygotic transcription. *Development* **137** (16), 2795–2804 (2010).

44. T. Lucas, *et al.*, Live imaging of bicoid-dependent transcription in Drosophila embryos. *Current biology* **23** (21), 2135–2139 (2013).

45. X.-J. Wang, Probabilistic decision making by slow reverberation in cortical circuits. *Neuron* **36** (5), 955–968 (2002).

46. D. Williams, *Probability with martingales* (Cambridge university press) (1991).

47. É. Roldán, *et al.*, Martingales for physicists: a treatise on stochastic thermodynamics and beyond. *Advances in Physics* **72** (1-2), 1–258 (2023).

48. I. Neri, Martingale approach for first-passage problems of time-additive observables in Markov processes. *Journal of Physics A: Mathematical and Theoretical* **58** (14), 145002 (2025).

49. C. W. Gardiner, Handbook of stochastic methods for physics, chemistry and the natural sciences. *Springer series in synergetics* (1985).

50. A. Wald, On cumulative sums of random variables. *The Annals of Mathematical Statistics* **15** (3), 283–296 (1944).

51. A. Dvoretzky, J. Kiefer, J. Wolfowitz, Sequential decision problems for processes with continuous time parameter. Testing hypotheses. *The Annals of Mathematical Statistics* **24** (2), 254–264 (1953).

52. A. C. Barato, É. Roldán, I. A. Martínez, S. Pigolotti, Arcsine laws in stochastic thermodynamics. *Physical review letters* **121** (9), 090601 (2018).

53. V. E. Foe, B. M. Alberts, Studies of nuclear and cytoplasmic behaviour during the five mitotic cycles that precede gastrulation in Drosophila embryogenesis. *Journal of cell science* **61** (1), 31–70 (1983).

Acknowledgments

IN conducted part of this research while visiting the Okinawa Institute of Science and Technology (OIST) through the Theoretical Sciences Visiting Program (TSVP). We thank A. Sassi for assistance with the visual perception experiment. We thank E. Kanemoto and G. Tripp for feedback on the experimental protocol.

Materials and Methods

Drift-diffusion: irrevocable decisions

We here present general mathematical results for the drift-diffusion model. We assume that the evidence is a linear function of the observation of the observation process X, and thus, for a given hypothesis, obeys the dynamics

$$\frac{dE}{dt} = a + b\,\xi(t). \tag{6}$$

We focus on equally likely hypotheses, so that $E(0) = 0$. We start by summarizing known results in the irrevocable case. Since the hypotheses are equally likely, we assume symmetric thresholds, $\ell_+ = \ell_- = \ell$. The probabilities of reaching the + and − thresholds are expressed by

$$p_+ = \frac{e^{\alpha\ell}}{1 + e^{\alpha\ell}} \qquad p_- = \frac{1}{1 + e^{\alpha\ell}}\,, \tag{7}$$

where $\alpha = 2a/b^2$. This result can be directly derived using that the process $M(t) = \exp(-\alpha E(t))$ is a martingale, and applying Doob's optional stopping theorem (*46–48*). The error probability η is given by the sum of the probabilities of false positives and false negatives:

$$\eta = \frac{p(+|-) + p(-|+)}{2} \tag{8}$$

In practice, the choice of the threshold ℓ is often based on the desired value of the error probability. For example, in the case of (2), (7) leads to

$$\ell = \frac{1}{2\gamma}\log\left(\frac{1-\eta}{\eta}\right)\,. \tag{9}$$

The distribution $p_{\rm ir}(t)$ of first-passage times can be obtained from the backward Kolmogorov equation (*49*):

$$p_{\rm ir}(t) = \frac{\pi b^2}{2\ell^2}\cosh\left(\frac{a\ell}{b^2}\right)\sum_{n=0}^{\infty}(-1)^n(2n+1)e^{-\frac{(2n+1)^2\pi^2 b^2 t}{8\ell^2} - \frac{a^2 t}{2b^2}}\,. \tag{10}$$

The average decision time is expressed by

$$\langle T_{\rm ir}\rangle = \frac{\ell(p_+ - p_-)}{a} = \frac{(1-2\eta)}{8\gamma^2}\log\left(\frac{\eta}{1-\eta}\right). \tag{11}$$

We note that the first equality is general and can be obtained using Wald's equation (*50, 51*), while the second equality is valid for the specific model of (2). (11) demonstrates the tradeoff relation $\langle T_{\rm ir}\rangle \sim -\ln(\eta)$ for small η. Results for the optimal case are recovered by setting $a = \pm\gamma_{\rm opt} = \pm 1/(2\sqrt{\tau})$ and $b = 1$.

Drift-diffusion: amendable decisions

We now move to the amendable case, for a general evidence process governed by (6). We directly consider the case in which decisions are taken within a finite time window $[0, t_\mathrm{f}]$. We start by defining the probability $S(\epsilon_E, t)$ that the process, starting from $E = \epsilon_E$ at time 0, does not reach $E = 0$ by time t. This probability is expressed by

$$S(\epsilon_E, t) = 1 - \frac{1}{2}\left[1 - \mathrm{erf}\left(\frac{|\epsilon_E|}{\sqrt{2b^2 t}} + \frac{a\epsilon_E\sqrt{t}}{\sqrt{2}b|\epsilon_E|}\right)\right] - \frac{e^{-2a\epsilon_E/b^2}}{2}\left[1 - \mathrm{erf}\left(\frac{|\epsilon_E|}{\sqrt{2b^2 t}} - \frac{a\epsilon_E\sqrt{t}}{\sqrt{2}b|\epsilon_E|}\right)\right], \tag{12}$$

where $\mathrm{erf}(x) = (2/\sqrt{\pi})\int_0^x e^{-t^2}\,\mathrm{d}t$ denotes the error function, see, e.g., Section (3.2.2) in Ref. (*39*). For small times, diffusion dominates, hence from $E = 0$ a fluctuation leads to $E = \epsilon_E$ or $E - \epsilon_E$ with equal probability. Conditioning to such fluctuation, we find

$$s(t) = \lim_{\epsilon_E \to 0^+} \frac{S(\epsilon_E, t) + S(-\epsilon_E, t)}{2\epsilon_E} = \frac{a}{b^2}\mathrm{erf}\left(\frac{a\sqrt{t}}{\sqrt{2}b}\right) + \sqrt{\frac{2}{\pi b^2 t}}e^{-a^2 t/(2b^2)}. \tag{13}$$

The finite-time decision time distribution is proportional to the probability of being in state $E = 0$, times the probability that the process will not return to the state $E = 0$ by time t:

$$p_\mathrm{am}(t|t_\mathrm{f}) = b^2\frac{e^{-\frac{a^2 t}{2b^2}}}{\sqrt{2\pi b^2 t}}s(t_\mathrm{f} - t)\,, \tag{14}$$

where the prefactor b^2 can be either justified by a dimensional argument, or by numerically verifying the normalization condition.

In finite-time, amendable decision entail a finite error probability. This probability is simply given by the probability that, at the final time, the sign of the evidence E is different than the sign of the bias a. Since the distribution of E is Gaussian at any time, we find

$$\eta = \frac{1}{2} - \frac{1}{2}\mathrm{erf}\left(\frac{a t_\mathrm{f}}{\sqrt{2b^2 t_\mathrm{f}}}\right). \tag{15}$$

In the limit $t_\mathrm{f} \to \infty$, we obtain the infinite-time results, i.e., a vanishing error probability and a distribution of decision times given by

$$p_\mathrm{am}(t) = \frac{|a|}{\sqrt{2\pi b^2 t}}\exp\left(-\frac{a^2 t}{2b^2}\right). \tag{16}$$

The corresponding average decision time is expressed by

$$\langle T_{\mathrm{am}} \rangle = \frac{b^2}{a^2}. \tag{17}$$

The optimal case discussed in the Results is recovered by setting $a = \pm\gamma_{\mathrm{opt}} = \pm 1/(2\sqrt{\tau})$ and $b = 1$. Another interesting limiting case of (14) is $a = 0$, in which the distribution of decision times reduces to $p_{\mathrm{am}}(t|E_0, t_{\mathrm{f}}) = 1/[\pi\sqrt{t(t - t_{\mathrm{f}})}]$. This result embodies the second arcsine law for Brownian motion (*52*).

Visual perception experiment: protocol

Eight volunteering participants were selected among students and researchers at OIST. Each participant repeatedly played a game in which a dot randomly moves on a computer screen, with the goal to assess whether the motion was biased towards the left or right direction and make decisions using the computer keyboard.

In the irrevocable version of the game, the game ended once a decision was taken, while in the amendable version participants could alter their decision, up to a time limit of 10s. For both types of games, participants were asked to decide rapidly while avoiding mistakes.

Each participant played eight groups of 30 games each. Four out of eight groups consisted of irrevocable games and the remaining four of amendable games. Irrevocable and amendable groups of games were played in an alternate fashion. Half of the participants started with an irrevocable group and half with an amendable group, to remove any potential bias. The four groups for each game involved an increasing level of difficulty. Specifically, we express as $(1/2 + q)$ and $(1/2 - q)$ the probabilities of moving in the direction of the bias or in the opposite direction, respectively, during a timestep $\Delta t = (1/60)$s of the game. The parameter q ranged in the set of values $q \in (0.15, 0.11, 0.07, 0.03)$ for the four games. The corresponding parameters of the observation process are $\mu_{\pm} = \pm 2q/\Delta t$ and $\sigma^2 = 1/\Delta t$. Participants were anonymized before the data analysis. The study protocol was approved by the OIST human subject research committee (reference number HSR-2024-016-2).

Visual perception experiment: data analysis

In the optimal (normative) model, we obtain the evidence rate from the drift and diffusion coefficients characterizing the dot motion: $\gamma = \gamma_{\rm opt} = 2q/\sqrt{\Delta t}$. This parameter fully specifies the optimal amendable model. For the optimal irrevocable model, we estimate the decision threshold ℓ from the average empirical error probability through (9).

In the descriptive model, the evidence rate is estimated from the experimental data. This estimate is different in the amendable and irrevocable cases. For amendable decisions, we combine (17) and (2), obtaining $\gamma = 1/\sqrt{\langle T_{\rm am}\rangle}$. This formula permits to easily estimate the evidence rate from the average decision time. For the hardest game ($q = 0.03$), we took finite-time effects into account to estimate the drift. This can be done either from the mean decision time (obtained by numerically integrating (14)) or from the error probability, (15). To be conservative, we took the smallest of these two values for each point. In the irrevocable case, we estimate the evidence rate by solving the expression of $\langle T_{\rm ir}\rangle$ and η for γ and ℓ. This procedure leads to $\gamma = \sqrt{\phi \tanh[\phi/2]/(2\langle T_{\rm ir}\rangle)}$ and $\ell = \sqrt{\phi\langle T_{\rm ir}\rangle/[2\tanh(\phi/2)]}$, where $\phi = \log[\eta/(1-\eta)]$.

Cellular sensing model

Our starting point is the equation governing the evidence

$$\frac{dE}{dt} = (j_- - j_+) + \ln\left(\frac{j_+}{j_-}\right)\frac{dN_\pm(t)}{dt} \tag{18}$$

for $j_+ > j_-$, see (*29*). Expressing j_- and j_+ in terms of ϵ and τ directly leads to (5).

For $E_0 = 0$ and $H = +$ we find the last passage time distribution

$$p_{\rm am}(t|H=+) = j_+(1 - e^{-\Delta(n+1-t/\tau_{\rm r})})e^{-j_+t}\frac{(j_+t)^n}{n!}\,, \tag{19}$$

where $\Delta = \ln j_+/j_- = \ln(1/[1-\epsilon])$, $\tau_{\rm r} = (\tau/\epsilon)\Delta$, and $t \in [n\tau_{\rm r}, (n+1)\tau_{\rm r}]$. For the negative hypothesis, we obtain

$$p_{\rm am}(t|H=-) = (1 - j_-\tau_{\rm r})\sum_{n=0}^{\infty} e^{-j_-t}\frac{(j_-t)^n}{n!}\delta\left(t - \tau_{\rm r}n\right)\,, \tag{20}$$

The average decision time for the negative hypothesis is expressed by

$$\langle T_{\rm am}|H=-\rangle = \frac{j_-\tau_{\rm r}^2}{(1-j_-\tau_{\rm r})^2}. \tag{21}$$

For the positive hypothesis, we could not find a simple expression for the average decision time. This time can be expressed by numerically integrating (19). Alternatively, the evidence process can also be approximated by a drift-diffusion process by a diffusion approximation of the counting process:

$$\frac{dN_\pm}{dt} \approx j_\pm + \sqrt{j_\pm}\xi(t)\,. \tag{22}$$

Using (17), we then find

$$\langle T_{\rm am}|H=\pm\rangle = \frac{j_\pm \ln^2(1-\epsilon)}{\left[j_\pm \ln(1-\epsilon)+\epsilon/\tau\right]^2}. \tag{23}$$

We note that, for the negative hypothesis, the continuous approximation of (23) exactly matches the solution given in (21). In contrast, for the positive hypothesis, (23) only approximates the numerically evaluated discrete distribution. (26) can be directly derived by approximating (5) as a drift-diffusion process using (22), and then computing the ratio of average times using (11) and (17).

We compute the mean irrevocable decision time $\langle T_{\rm irr}\rangle$ by applying again Wald's equation (*48, 50, 51*)

$$\langle T_{\rm ir}|H=\pm\rangle = \left\langle \frac{dE}{dt}\right\rangle (p_+\langle E(T)\rangle_+ - p_-\langle E(T)\rangle_-), \tag{24}$$

where

$$\left\langle \frac{dE}{dt}\middle| H=\pm\right\rangle = -\frac{\epsilon}{\tau} + j_\pm \ln\frac{1}{1-\epsilon}. \tag{25}$$

Neglecting overshoots, we approximate $\langle E(T)\rangle_+ = -\langle E(T)\rangle_- = \ell$. We have verified with simulations that Wald's equation yields a very good approximation when overshoots are neglected.

Averaging (23) and (24) over the two hypotheses and taking the ratio of the two times, we find that this ratio is independent of the accuracy:

$$\frac{\langle T\rangle_{\rm ir}}{\langle T\rangle_{\rm am}} \approx \frac{(1-2\eta)}{2}\ln\left(\frac{1}{\eta}-1\right)\,. \tag{26}$$

Bicoid-Hunchback model

We describe the Bicoid concentration gradient as

$$c(x) = c_0 e^{-\lambda(x-x_{\rm m})}, \tag{27}$$

see (*10, 30, 42*), where $x \in [0,1]$ denotes the relative position along the anterior-posterior axis (where $x=0$ is the anterior pole and $x=1$ the posterior pole, corresponding to about $500\mu m$),

$\lambda = 5$ is the decay length of the concentration profile and $c_0 = 4.8 \pm 0.6\mu m^{-3}$ is the Bicoid concentration at the mid point $x_m \approx 0.45$ where the Hunchback profile switches from high to low during nuclear cycle 10 (*10,43*). We estimate the distance between neighboring nuclei as $\Delta x = 0.02$.

Due to the reproducibility of the midpoint x_m across embryos, and due to the sharp decline of the Hunchback expression profile at the midpoint, we assume that the two hypotheses correspond to two Bicoid concentrations close to the Hunchback boundary, separated by one nucleus diameter: $c_+ = c(x_\mathrm{m})$ and $c_- = c(x_\mathrm{m} + \Delta x)$. This choice corresponds to a precision $\epsilon = (c_+ - c_-)/c_+ = 0.1$ and a timescale $\tau = 20\,\mathrm{s}$. Our model is then expressed by

$$\frac{dE(x,t)}{dt} = -\frac{\epsilon}{\tau} + \ln\left(\frac{1}{1-\epsilon}\right)\frac{dN(x,t)}{dt}\,, \tag{28}$$

see (5), where $N(x,t)$ is a Poisson point process in t of rate $j(x) = 4\pi r D c(x)$. We take $D = 0.3(\mu m)^2/s$ and $r = 3\mathrm{nm}$, as in Ref. (*30*).

We consider the model dynamics up to a finite time $t_\mathrm{f} = 5.5$ min, representing the time that a discrete nuclear envelope is observed during nuclear cycle 10, see Table 1 in Ref. (*53*). The reason is the nuclear envelope breaks down, so that the Bicoid concentration drastically decreases, at the end of each cycle (*30*).

The probability p_Hb to express Hunchback is given by the probability that the evidence process is positive at time t_f. Using that $N(x,t)$ is a Poisson random variable, we obtain

$$p_\mathrm{Hb}(x) = 1 - e^{-t_\mathrm{f} j(x)} \sum_{n=0}^{n_{t_\mathrm{f}}} \frac{(t_\mathrm{f} j(x))^n}{n!}\,, \tag{29}$$

with $n_{t_\mathrm{f}} = \lfloor t_\mathrm{f}(j_+ - j_-)/\ln(j_+/j_-)\rfloor$.